Coexpression of ΔNp63/p40 and TTF1 Within Most of the Same Individual Cells Identifies Life-Threatening NSCLC Featuring Squamous and Glandular Biphenotypic Differentiation: Clinicopathologic Correlations

Giuseppe Pelosi, MD, MIAC,[a,b,*] Matteo Bulloni, PhD,[c] Martina Vescio, PhD,[c]
Silvia Uccella, MD,[d] Fabien Forest, MD,[e] Giorgia Leone, MD,[f] Massimo Barberis, MD,[g]
Daoud Rahal, MD,[h] Paola Bossi, MD,[h] Giovanna Finzi, MD,[d] Deborah Marchiori, MD,[d]
Marco De Luca, MD,[d] Fausto Sessa, MD,[d] Sergio Harari, MD,[i,j] Manuela Spinelli, MD,[k]
Patrizia Viola, MD,[l] Paolo Macrì, MD,[m] Stefania Maria, MD,[m] Antonio Rizzo, MD,[f]
Antonio Picone, MD,[n] Linda Pattini, PhD[c]

[a]Department of Oncology and Hemato-Oncology, University of Milan, Milan, Italy
[b]Inter-Hospital Pathology Division, Istituto di Ricovero e Cura a Carattere Scientifico (IRCSS) MultiMedica, Milan, Italy
[c]Department of Electronics, Information and Bioengineering, Politecnico di Milano, Milan, Italy
[d]Pathology Unit, Department of Medicine and Surgery, University of Insubria, Varese, Italy
[e]Department of Pathology, University Hospital Center (CHU), North Hospital, Saint Etienne, France
[f]Pathology Service, Humanitas Istituto Clinico Catanese, Catania, Italy
[g]Histopathology and Molecular Diagnostics Unit, Istituto di Ricovero e Cura a Carattere Scientifico (IRCSS) European
Institute of Oncology, Milan, Italy
[h]Department of Pathology, Humanitas Clinical and Research Center, Istituto di Ricovero e Cura a Carattere Scientifico
(IRCSS), Milan, Italy
[i]Department of Medical Sciences and Community Health, University of Milan, Milan, Italy
[j]Division of Pneumology, San Giuseppe Hospital, Istituto di Ricovero e Cura a Carattere Scientifico (IRCSS) MultiMedica,
Milan, Italy
[k]Cellular Pathology Department, Worcester Royal Hospital, Worcester, United Kingdom
[l]Cellular Pathology Department, Hammersmith Hospital, London, United Kingdom
[m]Division of Oncologic Thoracic Surgery, Humanitas Istituto Clinico Catanese, Catania, Italy
[n]Department of Oncology, Humanitas Istituto Clinico Catanese, Catania, Italy

ABSTRACT

Introduction: Double occurrence of TTF1 and ΔNp63/p40 (henceforth, p40) within the same individual cells is exceedingly rare in lung cancer. Little is known on their biological and clinical implications.

Methods: Two index cases immunoreactive for both p40 and TTF1 and nine tumors selected from The Cancer Genome Atlas (TCGA) according to the mRNA levels of the two relevant genes entered the study.

Results: The two index cases were peripherally located, poorly differentiated, and behaviorally unfavorable carcinomas, which shared widespread p40 and TTF1 decoration within the same individual tumor cells. They also retained SMARCA2 and SMARCA4 expression, while variably stained

for p53, cytokeratin 5, and programmed death-ligand 1. A subset of basal cells p40+/TTF1+ could be found in normal distal airways. Biphenotypic glandular and squamous differentiation was unveiled by electron microscopy, along with *EGFR*, *RAD51B*, *CCND3*, or *NF1* mutations and *IGF1R*, *MYC*, *CCND1*, or *CDK2* copy number variations on next-generation sequencing analysis. The nine tumors from TCGA (0.88% of 1018 tumors) shared the same poor prognosis, clinical presentation, and challenging histology and had activated pathways of enhanced angiogenesis and epithelial-mesenchymal transition. Mutation and copy number variation profiles did not differ from the other TCGA tumors.

Conclusions: Double p40+/TTF1+ lung carcinomas are aggressive and likely underrecognized non–small cell carcinomas, whose origin could reside in double-positive distal airway stem-like basal cells through either de novo-basal-like or differentiating cell mechanisms according to a model of epithelial renewal.

Introduction

Two master regulators of lung cancer development, namely ΔNp63/p40 (henceforth, p40) and TTF1, are widely used in diagnostic algorithms to distinguish adenocarcinoma (ADC) and squamous cell carcinoma (SQC).[1-4] The phenotype p40+/TTF1− corresponds to SQC, and the reverse to ADC and double negativity (as found in approximately 20% of instances) supports the diagnosis of non–small cell carcinoma—not otherwise specified (NSCC-NOS) and large cell carcinoma (LCC) in biopsy/cytology and surgical specimens, respectively.[1-4] Coexpression of both biomarkers within the same individual tumor cells is an exceedingly rare occurrence (<1% of NSCC), with only three single cases[5-7] (Table 1) and sparse anecdotal instances, either blurred in large tumor series[3,8] or presented in abstract form only,[9] being thus far on record. This bewildering phenotype is currently classified as ADC or NSCC-NOS/LCC, favoring ADC, because of the prevalence of TTF1 over any squamous biomarkers.[10-13] Little is known, however, on the ultrastructural traits (just one case is available thus far[5]), molecular alterations, biological functions, and clinical outcome of such an uncommon tumor phenotype.

This study was aimed to thoroughly investigate two additional instances of p40+/TTF1+ NSCC we encountered in our pathology practice to unravel the clinical, immunohistochemistry (IHC), electron microscopy (EM), and next-generation sequencing characteristics of such an uncommon phenotype. Furthermore, The Cancer Genome Atlas (TCGA) was explored to identify similar tumors, which were selected according to the mRNA levels of the two relevant genes, for clinical and molecular comparison.

Materials and Methods

Index Cases

Case number 1 referred to a 62-year-old woman, former smoker (10 pack-years), who had quit 30 years earlier. A diagnosis of ADC was preoperatively done in bronchoscopy biopsy, whereas computed tomography scan revealed multiple nodules in the right lung (Fig. 1*A*). On resection, an ADC (4.5 cm in diameter) was confirmed with the same phenotype, which was staged pT4N2 (IIIB, according to the Union for International Cancer Control/American Joint Committee on Cancer eighth edition) because of intrapulmonary and mediastinal lymph node metastases (Fig. 1*A* inset). Despite the *EGFR del19* mutation, the patient underwent chemotherapy, and gefitinib treatment was added 1 year after because of brain metastases. Progression of brain metastases and new bone colonization were managed by osimertinib mesylate, but the patient condition progressively worsened and she died 48 months after her initial cancer diagnosis.

Case number 2 concerned a 62-year-old man, former smoker (23 pack-years), who had quit 30 years earlier. A 4.7-cm-sized SQC was diagnosed on bronchoscopy (just p40 was originally performed), whereas computed tomography scan revealed a tumor mass on the left lower lobe (Fig. 1*B*). After neoadjuvant chemotherapy, a LCC positive for p40 and TTF1 was identified and staged ypT2bN2 (yIIIA) because of hilar and mediastinal lymph node involvement (Fig. 1*B*). Early thoracic and liver relapse were subsequently treated with chemotherapy plus pembrolizumab, but the patient experienced progressive disease and he died 3 months after his initial diagnosis.

Compliance With Ethical Standards

Both patients had provided informed consent to the personal data processing at hospital admission.

Immunohistochemistry

Antibodies for p40 (clone BC28), TTF1 (clone 8G7G3/1), p53 (clone DO7), cytokeratin 5 (clone SP27), SMARCA2 (clone BRM/D9E8B), SMARCA4 (clone EPN-CIR111A), programmed death-ligand-1 (PD-L1) (clone SP263), synaptophysin (clone SP11), and chromogranin A (clone LK2H10) made up the diluted reagents from

Table 1. Clinicopathologic Information on the Three Literature Cases With p40+/TTF1+ Phenotype

Reference Number	Author	Sex/Age (y)	Smoker/Pack-Year	Site	Size (cm)	Pleural Effusion	Tumor Metastasis	Tumor Stage	Type of Material	Final Diagnosis	IHC Profile	Antibodies	Gene Alterations (% of Allelic Frequency or CNV)	PD-L1 Status as TPS	Electron Microscopic Findings	Clinical Outcome	Medical Therapy
#-5	Pelosi et al. (2015)[5]	M/77	Former/40	Left lung, hilar mass	8.5	Yes	Mediastinal LNs	c-IVA	Bronchial biopsy	NSCC-NOS with adenosquamous phenotype	p40+/TTF1+ in most tumor cells	TTF1: 8G7G3/1 p40: BC28	KRAS (32%) & TP53 (71%) mutations; FGFR1 (7.1 CNV) amplification	N.A.	Glandular lineage: extracellular lumen formation with microvilli-like protrusions; Squamous lineage: abundant perinuclear tonofilaments	Died of disease one month and a half after the initial diagnosis	None
#-6	Hayashi et al. (2018)[6]	M/73	Former/141	Left upper lobe	1.9	No	N.A.	N.A.	Lobectomy	Adenosquamous carcinoma	p40+/TTF1+ in most tumor cells	TTF1: 8G7G3/1 p40: BC28	PTEN (11%) TP53 (9.6%)	N.A.	N.A.	N.A.	N.A.
#-7	Spinelli et al. (2019)[7]	M/51	Current/N.A.	Right upper lobe	3.1	No	Mediastinal LNs, brain, bone, adrenal glands	c-IVB	Lung core biopsy	NSCC-NOS with hints to squamous differentiation	p40+/TTF1+ in most tumor cells	TTF1: SPT24 p40: polyclonal rabbit antibody	TP53 polymorphism c.215C>G (p.Pro72Arg)	70%	Not performed	Died of disease three months after the initial diagnosis	Radiotherapy to brain metastases with some symptomatic relief

#, number; CNV, copy number variation; LN, lymph node; N.A., not available; NSCC-NOS, non-small cell carcinoma—not otherwise specified; PD-L1, programmed death-ligand 1; TPS, tumor proportion score.

Ventana-Roche Group, Basel, Switzerland. All antibodies were developed with horseradish peroxidase and 3-3′-diaminobenzidine (DAB) to obtain a brown end product of staining. Concurrent double reaction was obtained with horseradish peroxidase-DAB for TTF1 followed by universal alkaline phosphatase red detection kit (Ventana) for p40. An automated immunostainer (Benchmark ULTRA IHC/ISH System, Ventana-Roche Group) with OptiView (p40, S263) or ultraView (TTF1, p53, cytokeratin 5) DAB IHC detection kit (Ventana-Roche Group) was used for all reactions. Additional Alcian blue stain was performed for case number 2 only.

Electron Microscopy

Paraffin-retrieved tissue for both index cases was routinely processed for EM analysis and eventually examined on a Morgagni 268D Transmission Electron Microscope (Philips, Eindhoven, The Netherlands).

Molecular Analysis

Next-generation sequencing was carried out in the two index cases using Oncomine Comprehensive Assay v3 (Thermo-Fisher Scientific Inc., Waltham, MA), which allows the detection of single-nucleotide variants, copy number variations (CNVs), gene fusions, and insertion/deletions from 161 cancer genes. Only single-nucleotide variants with variant allele frequency greater than or equal to 5% and adequate quality metrics (read depth >100; variant allele frequency $\times$ read depth >25, $p = 0.00001$) were reported.[14] CNVs were evaluated for samples with a median of the absolute values of all pairwise difference less than 0.5.[15]

TCGA Analysis

Isoform expression data were retrieved from Fire-Browse (http://firebrowse.org/) for 517 ADCs and 501 SQCs. TTF1 and p40 expression levels were assessed by summing the prevalence levels of all the corresponding isoforms (ΔNp63α [uc003fsc.2], ΔNp63β [uc003fsd.2], ΔNp63γ [uc003fsb.2], and ΔNp63ε [uc010hzd.1] for p40; uc001wtt.2, uc001wtu.2, and uc001wtv.2 for TTF1). Positivity criteria were devised for p40 according to the numerical mRNA thresholds which best classified tumors as ADC or SQC by means of the following rule: (p40 level) > threshold$_{\text{p40}}$ → SQC, (p40 level) $\leq$ threshold$_{\text{p40}}$ → ADC. The same procedure was carried out separately for TTF1, considering (TTF1 level) > threshold$_{\text{TTF1}}$ → ADC, (TTF1 level) $\leq$ threshold$_{\text{TTF1}}$ → SQC. According to the originally proposed diagnoses, the p40 thresholds obtained through this procedure correctly classified 500 of 517 (96.7%) ADCs and 449 of 501 (89.6%) SQCs (accuracy = 93.2%), whereas the
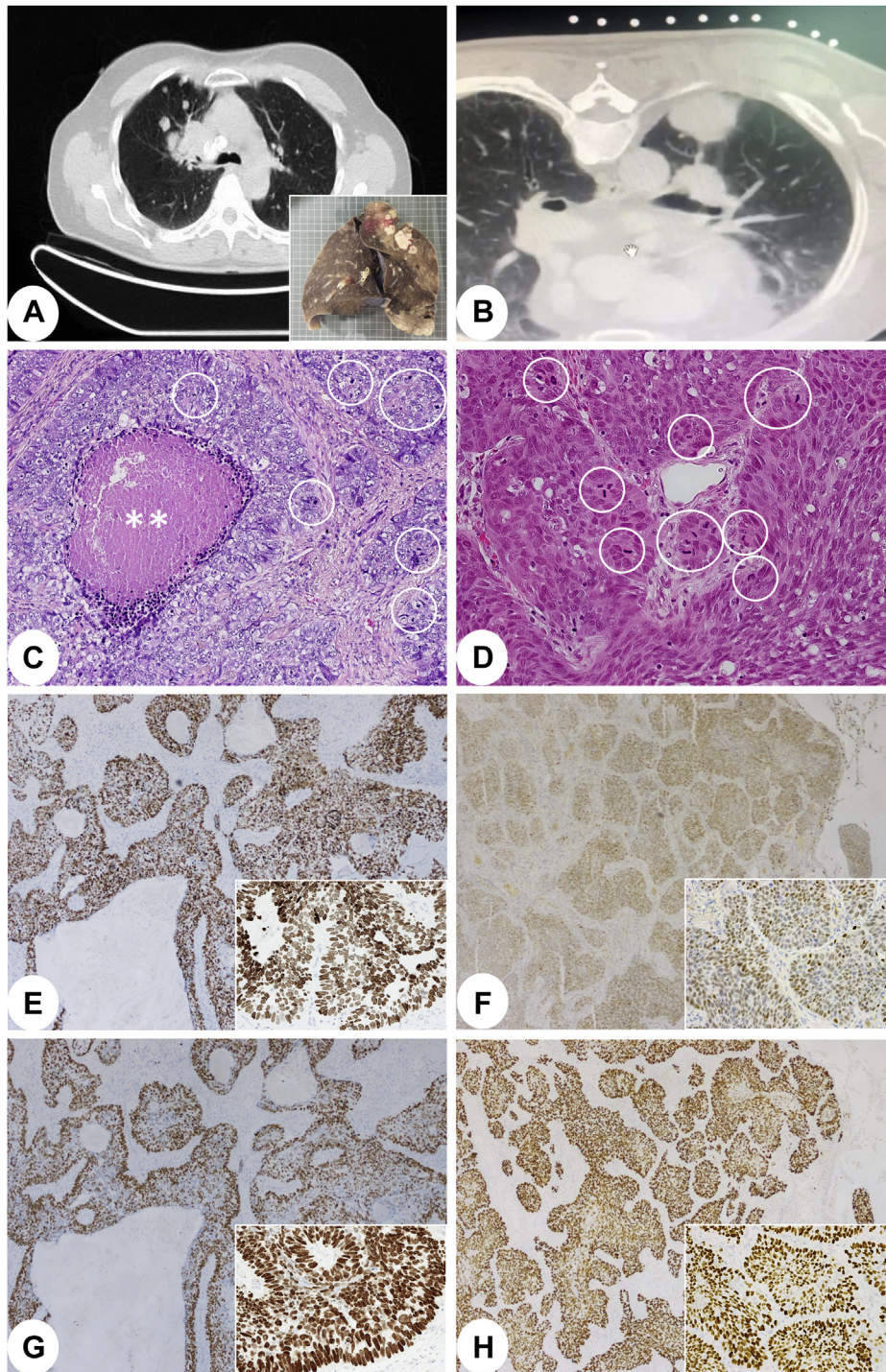
Figure 1. (*A-F*) Histologic pictures of the two index cases (on the left, case #1 *A, C, E, G*; on the right, case #2 *B, D, F, H*). CT scan (*A*) and gross pathology (*A,* inset) of case #1, which featured poorly differentiated carcinoma with comedo-type necrosis and peripheral palisading (*C*). There was concurrent TTF1 (*E* and *E* inset) and p40 (*G* and *G* inset) immunoreactivity within most of the same individual tumor cells. Similarly, case #2 presented with a large tumor on CT scan (*B*), which featured some resemblance to squamous differentiation despite the lack of horn pearls and intercellular bridges (*D*). Even this tumor case exhibited widespread and consistent positivity for TTF1 (*F* and *F* inset) and p40 (*H* and *H* inset) in most tumor cells. Histologic picture magnification was ×200 for *C* to *H* panels and ×40 for *E-H* insets. #, number; CT, computed tomography.

corresponding TTF1 threshold classified 452 of 517 (87.4%) ADCs and 458 of 501 (91.4%) SQCs (accuracy = 89.4%). Double-positive tumors were thus identified as those fulfilling both positivity criteria and displaying similar absolute values of expression (<10% difference between the two). Differential expression

analysis of mRNAs was performed on gene expression data from FireBrowse by means of DESeq2 software. (https://bioconductor.org/packages/release/bioc/html/DESeq2.html). Functional enrichment analysis was carried out on the resulting output by means of Gene Set Enrichment Analysis software (https://www.gsea-msigdb.org/gsea/index.jsp). Clinicopathologic data, including overall survival, were available for 1003 patients (508 ADCs, 495 SQCs) on cBioPortal for cancer genomics (https://www.cbioportal.org/): two patients with two tumor samples each were excluded from the survival analysis. CNV and somatic mutation data were retrieved from the University of California—Santa Cruz—XenaBrowser (https://xenabrowser.net/) for 1010 (512 ADCs, 498 SQCs) and 986 (509 ADCs, 477 SQCs) tumors, respectively.

Statistical Analysis

Kaplan-Meier and log-rank methods were used for the survival analysis.

Mutation and CNV enrichments were evaluated by means of two-tailed Fisher exact test. p values were corrected according to Bonferroni (mutations and CNV) or Benjamini-Hochberg (differential expression and Gene Set Enrichment Analysis) correction. A p value less than 0.05 was set as significance level.

Results
Index Cases

The tumors featured LCC with comedo-type necrosis and peripheral palisading (Fig. 1C) or vaguely resembled squamous differentiation but with no evidence of horn pearls or intercellular bridges (Fig. 1D). Plentiful mitoses were recognizable (Fig. 1C and D, white circles). There was no increase of tumor-infiltrating lymphocytes. IHC study revealed diffuse decoration for both TTF1 (Fig. 1E and F) and p40 (Fig. 1G and H) within most of the same individual tumor cells. Additional IHC revealed diffuse reactivity for p53 and erratic cytokeratin 5 decoration in case number 1, whereas the reverse phenotype occurred in case number 2. SMARCA2 and SMARCA4 were both retained (Supplementary Fig. 1 A–F). Tumor proportion score for PD-L1 was negative in case number 1 or revealed a 2% value in case number 2 (pictures not provided). No tumor cells were reactive for neuroendocrine differentiation markers. In normal peripheral airways of the two index cases, there was a subset of basally located bronchiolar cells revealing double p40+/TTF1+ phenotype (Supplementary Fig. 2A–C). Preoperative biopsy results revealed shared TTF1 and p40 decoration within most of the same tumor cells (Supplementary Fig. 3A–D).

Biphenotypic properties with concomitant evidence of glandular and squamous differentiation in the same tumor cells emerged from the EM study in either case (Fig. 2A and B). Glandular differentiation was heralded by intercellular (case number 1; Fig. 2A) and intracellular (case number 2; Fig. 2B) lumina along with cytoplasmic granules similar to those of club cells. Squamous features were in turn embodied by intracytoplasmic dense fascicles of keratin fibers, close to cell membranes, to realize desmosomes (Fig. 2A and B). Focal Alcian blue-positive mucin stain was also found in case number 2 (Fig. 2B, inset).

Molecular testing results revealed *EGFR*, *TP53*, *RAD51B*, and *CCND3* mutations along with CNVs for *IGF1R*, *MYC*, *CCND1*, and *CDK2* in case number 1 and standalone *NF1* mutation in case number 2. Fusion genes were not assessed in case number 1 for poor quality of mRNA, whereas they were absent in case number 2. CNV analysis was not informative in case number 2 for technical reasons. Summarized molecular results along with clinicopathologic characteristics of the two index cases are found in Table 2.

TCGA Analysis

The nine tumors recruited from TCGA accounted for 0.88% of 1018 TCGA carcinomas, with original diagnoses of ADC in two cases and SQC in seven cases (Supplementary Table 1). An accurate morphologic reevaluation of all images available on TCGA for these nine tumors excluded the possibility of facing with adenosquamous carcinomas (ADSQCs). Survival curves revealed only a trend for unfavorable clinical outcome ($p = 0.18$), likely owing to the small sample size (Fig. 3). There were 53 deregulated genes in this tumor subset (Supplementary Table 2), whereas gene set enrichment yielded 147 up-regulated and 124 down-regulated pathways (Supplementary Table 3A and B). These identified functional signatures are consistent with biological aggressiveness, such as enhanced angiogenesis and epithelial-mesenchymal transition. Enrichment analyses for somatic mutations and CNVs did not identify statistically significant differences in these nine tumors as compared with the remaining TCGA series.

Discussion

Coexpression of p40 and TTF1 within most of the same individual tumor cells is exceedingly rare in lung cancer (Table 1).[5-7] This is likely because the differentiation programs leading to the development of SQC (under *p63* gene) or ADC (under *TTF1* gene) are mutually exclusive, when one gene transcriptionally prevails over the other.[1-3] Even ADSQC in geographically separate
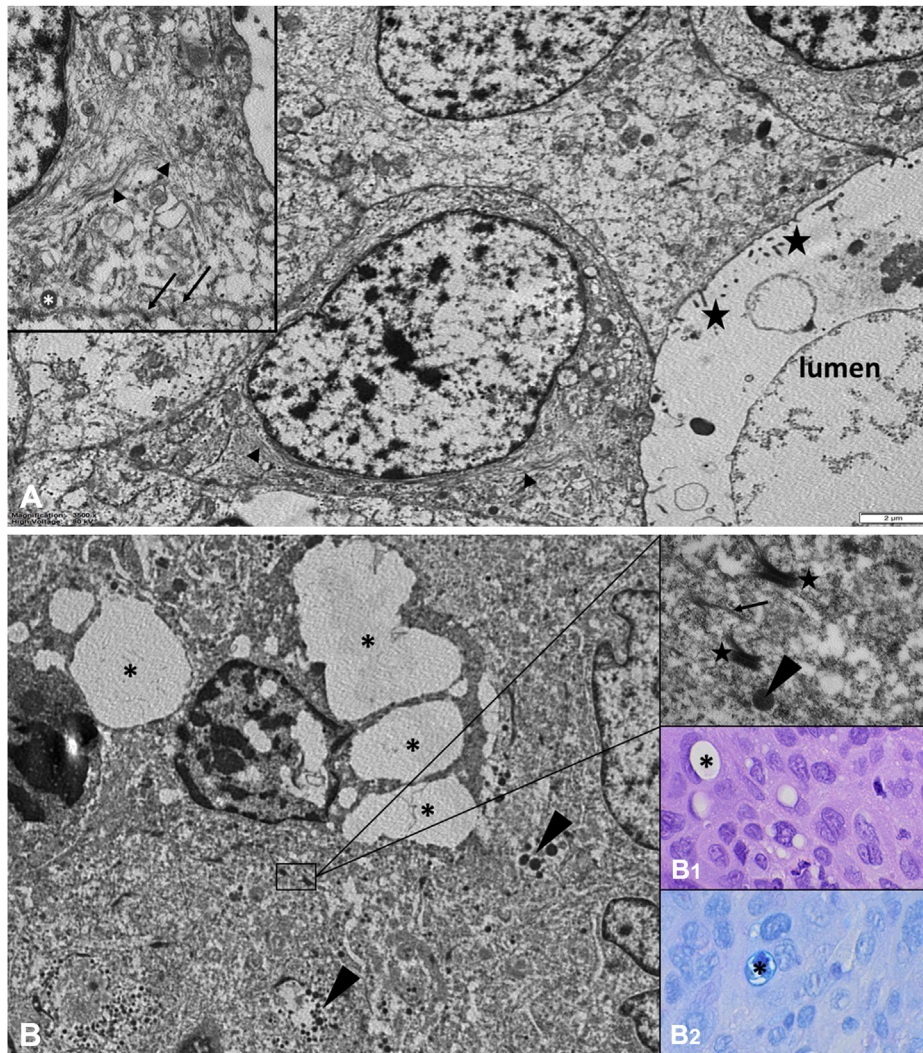
Figure 2. (*A, B*) The ultrastructural study revealed in case #1 (*A*), intercellular lumina bordered by microvilli (black stars) and fascicles of keratin fibers (black arrowheads, also in the inset). Higher magnification (inset) of the same case revealed club cell granule (white asterisk) and desmosomes (black arrows) (electron microscopy magnification: ×3500 and ×8900, respectively). In case #2 (*B*), there were intracytoplasmic lumina (black asterisks), club cell-like granules (black arrowhead, also in the upper inset), and fascicles of keratin fibers (upper inset, black arrow), which condensed themselves into desmosomes (upper inset, black stars). Intracellular lumina were also observed at light microscopy (B₁, middle inset, black asterisk), which were filled by Alcian blue-reactive mucin droplets (B₂, lower inset, black asterisk). Electron microscopy magnification: ×3500 and ×28,000, respectively; hematoxylin and eosin: ×630; Alcian blue stain: ×630. #, number.

tumor regions, few ADC or LCC in less than 10% tumor cells,[2-4] SQC foci in ALK-translocated ADC,[16] or SQC displaying ALK[17] or ROS1 translocation[18] or EGFR[19,20] mutation may be concurrently positive for p40 and TTF1, but again in a mutually exclusive manner. In this regard, the diffuse positivity for both biomarkers within most of the same individual tumor cells ruled out the occurrence of ADSQC. The extreme rarity of the double phenotype of p40+/TTF1+ we herein document after reporting the first case in literature[5] is likely owing to the challenging position of these tumors on the inflection point of two mutually exclusive differentiation programs,

thereby realizing biphenotypic tumors that feature simultaneous glandular and keratinizing codifferentiation (Fig. 2*A* and *B*). This p40/TTF1 coexpression resulted in clinically unfavorable tumors (Fig. 3 and Table 1), likely owing to unsuccessful therapy and aggressiveness in molecular pathway activation, such as enhanced angiogenesis and epithelial-mesenchymal transition (Supplementary Table 2 and Supplementary Table 3*A* and *B*). It is tempting to speculate that the nine tumors selected from TCGA on the basis of mRNA levels of the relevant genes well reflected the two index cases, inasmuch as shared similar traits such as

Table 2. Next-Generation Sequencing Results and Clinicopathologic Characteristics of the Two Index Cases Under Evaluation

Tumor case	Sex/Age (y)	Smoker/Pack-Year	Site	Size (cm)	Pleura Effusion	Tumor Metastasis	Type of Material	Tumor Stage	Metastasis Over Time	Clinical Outcome (mo)	Medical Therapy	Gene Mutations (% of Allelic Frequency)	Gene (Level of Copy Number Variation)	Fusion Genes
#-1	W/62	Former/10	Upper right lobe	4.5	No	Intralung Mediastinal LN	Biopsy sample and resection specimen	IIIB	Brain	DOD 48 mo	CT Osimertinib	EGFR, p.Glu746_ALA750del, c.2235_2249del (61%); TP53 p.Glu224Asp, c.672G>T (53%); VUS: RAD51B, p.Pro365Arg, c1094C>G (41%) and CCND3, p.Ser259Ala, c775T>G (47%)	IGF1R: 56.05 MYC: 28 CCND1: 10.93 CDK2: 5.95	Not assessable for poor quality of mRNAs
#-2	M/62	Former/23	Left lower lobe	4.7	No	Hilar & mediastinal LN	Biopsy sample and resection specimen	YIIIA	Thorax Liver	DOD 3 mo	CT Pembrolizumab	NF1, pArg1769Ter, c.5305C>T (54%)	Not assessable for technical reasons	None

#, number; CT, chemotherapy; DOD, died of disease; LN, lymph nodes; M, male; VUS, variant of uncertain significance; W, woman.

challenging morphology, clinical presentation, and ultimate poor outcome (Supplementary Table 1 and Fig. 3). An accurate morphologic reevaluation of all images available on TCGA for these nine tumors excluded the possibility of facing with ADSQCs, potentially responsible for double increment of p40 and TTF1 mRNAs.

The double expression of p40/TTF1 at the level of the same individual tumor cells had a normal counterpart in bronchiolar basal cells (Supplementary Fig. 2*A* and *B*) of the same index cases, which could be consistent with an origin from a subset of distal airway stem-like basal cells. These cells sharing p40 and TTF1 expression have been reported to produce bronchiole-like and alveolus-like organoids in experimental murine models.[21] The peripheral location of our cases (Fig. 1*A* and *B*), their poor differentiation mimicking either basaloid squamous or uncommitted surface bronchial cells (Fig. 1*C* and *D*), and the occurrence of gene alterations and CNVs common to either ADC (e.g., *EGFR*, *NF1*, *TP53*, *IGF1R*) or SQC (e.g., *NF1*, *TP53*, *CCND1*, *IGF1R*, *CCND3*)[22-25] (Table 2) are likely to suggest an origin from a subset of p40+/TTF1+ stem-like basal cells normally existing in distal airways (Supplementary Fig. 2*A* and *C*). Decoration for cytokeratin 5 (a basal cell biomarker induced in the lung by *p63* gene[26]) was obvious in case number 2 more hinting at basaloid keratinizing cells, whereas it was negligible in the gland-looking case number 1. Conversely, *TP53* mutation and protein overexpression were private to case number 1 (more resembling uncommitted bronchial surface gland-like cells), as this gene alteration prevails in bronchial epithelium branch-derived ADC[27] (Supplementary Fig. 1*A–F*). These findings were consistent with a model of de novo-basal-like carcinomas with unbalanced glandular and squamous codifferentiation, respectively, on functional recruitment of *p63* and *TTF1* master genes in double-positive progenitor cells (Fig. 4). This model was assonant with epithelial renewal mechanisms normally acting in the lung and somewhat realized some similarity to the development of triple-negative breast carcinomas, wherein there are consistent features of luminal-like and basal-like codifferentiation.[28,29] Although we cannot completely exclude that dedifferentiation or reprogramming could be responsible for these uncommon NSCLCs to share TTF1 and p40 expression, codifferentiation on rare double-positive basal stem cells should better account for the extreme rarity of this phenotype, in our opinion.

SMARCA2 and SMARCA4 gene products were both retained, and this phenotype could have contributed to chemotherapy failure and immune system anergy,[30] also exemplified by scantness of tumor-infiltrating lymphocytes, PD-L1 negativity, ineffectiveness of pembrolizumab
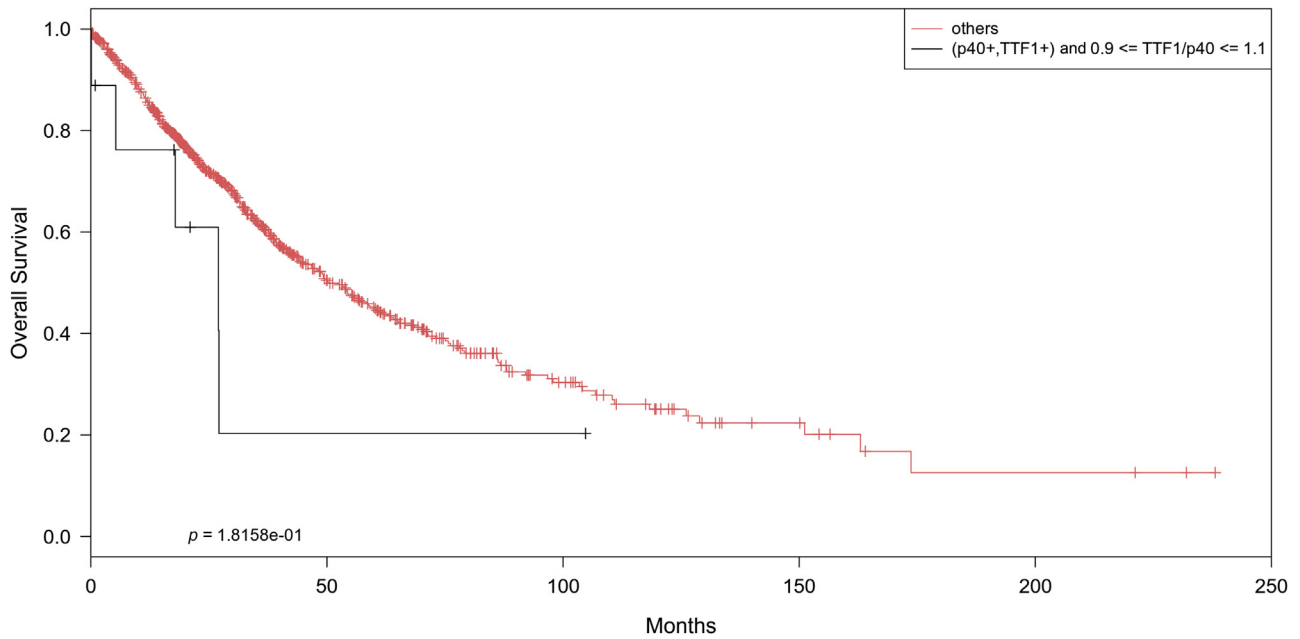
Figure 3. Survival curve of the nine carcinomas with double p40+/TTF1+ phenotype revealed a trend for poor clinical outcome as compared with the remaining TCGA tumor series, which are labeled as "others" in the upper legend. TCGA, The Cancer Genome Atlas.
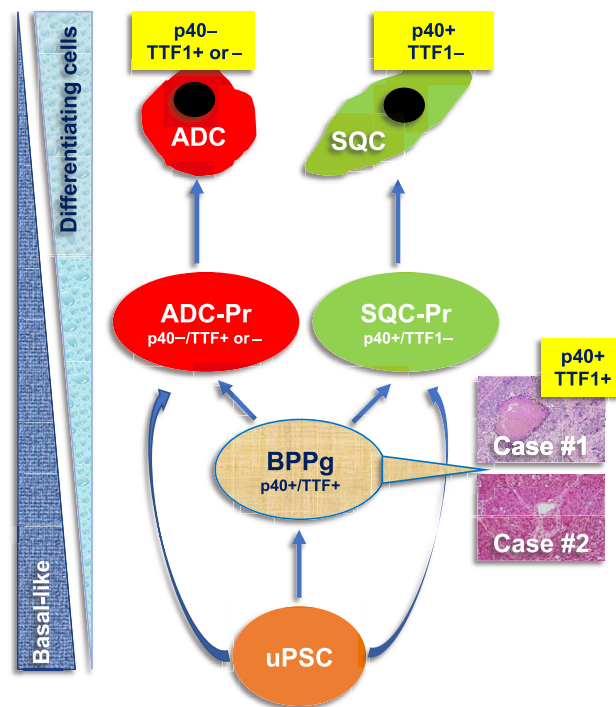
Figure 4. Interpretation model on the development of double p40+/TTF1+ tumors from a subset of bronchiolar basal cells present in normal distal airways, which share reactivity for both TTF1 and p40. This model is based on the turnover of the normal epithelium, where uPSC, putatively aligned along the basal layer, is likely to give rise to BPPg positive for both p40 and TTF1 (horizontal or de novo-basal-like propagation) thanks to their asymmetrical self-renewal properties and differentiating precursors already committed to specific cell lineages (vertical or differentiating cell evolution), including ADC-Pr with phenotype p40 and TTF1 either positive or negative and SQC-Pr with phenotype p40+/TTF1−. Note that there is an inverse relationship between basal-like differentiation imprinted by stem/precursor cells and differentiating cells paralleling lineage-specific precursors. #, number; ADC, adenocarcinoma; ADC-Pr, adenocarcinoma precursor; BPPg, bipotential progenitor; SQC, squamous cell carcinoma; SQC-Pr, squamous cell carcinoma precursor; uPSC, uncommitted pulmonary stem cell.

(case number 2), or mutanome-derived low neoantigens of the EGFR-altered case number 1.[31,32] Furthermore, resistance to EGFR tyrosine kinase inhibitor could have derived from alternative signaling coactivation through *IGFR1*,[33] *MYC*,[34] *CCND1*,[35] or *CDK2* CNVs, also conferring worse prognosis through *TP53* inactivation.[34,36]

Double p40+/TTF1+ tumors in the lung have been purportedly classified, in the past, as ADC, NSCC with adenosquamous immunophenotype, NSCC-NOS, LCC-favor ADC, or even SQC, depending on the different morphologic impressions, IHC biomarkers, or different tool interpretation.[3,5-8,10-13] We feel that NSCC-NOS or LCC with biphenotypic glandular and keratinizing biphenotypic differentiation could be a valuable compromise to label this underrecognized and new entity, with a comment on its own unusual phenotype, enhanced clinical aggressiveness, poor prognosis, and disappointing resistance to treatments.

CRediT Authorship Contribution Statement

Giuseppe Pelosi: Conceptualization, Data curation, Formal analysis, Investigation, Methodology, Supervision, Validation, Writing—original draft, Finalization of the manuscript.

Matteo Bulloni: Performance of bioinformatic analysis, Data curation, Investigation, Drafting, Finalization of the manuscript as young researcher.

Martina Vescio: Participation in the team research activity as an active member, Data curation, Investigation, Drafting, Finalization of the manuscript.

Silvia Uccella, Giovanna Finzi, Deborah Marchiori: Performance of the electron microscopy study, Drafting, Finalization of the manuscript.

Massimo Barberis: Performance of the next-generation sequencing analysis, Drafting, Finalization of the manuscript.

Fabien Forest, Giorgia Leone: Provided the two cases under evaluation, Critical revision, Finalization of the manuscript.

Fabien Forest: Provided the preoperative biopsy sample of index case number 2.

Paola Bossi: Provided the preoperative biopsy sample of index case number 2, Critical revision, Finalization of the manuscript.

Daoud Rahal, Marco De Luca, Fausto Sessa, Sergio Harari, Manuela Spinelli, Patrizia Viola, Paolo Macrì, Stefania Maria, Antonio Rizzo, Antonio Picone: Critical revision, Finalized the manuscript.

Linda Pattini: Conceptualization, Data curation, Investigation, Methodology, Supervision, Writing—original draft, Finalization of the manuscript.

Supplementary Data
Note: To access the supplementary material accompanying this article, visit the online version of the *JTO Clinical and Research Reports* at www.jtocrr.org/ and at https://doi.org/10.1016/j.jtocrr.2021.100222.

References

1. Bishop JA, Teruya-Feldstein J, Westra WH, Pelosi G, Travis WD, Rekhtman N. p40 (ΔNp63) is superior to p63 for the diagnosis of pulmonary squamous cell carcinoma. *Mod Pathol*. 2012;25:405-415.
2. Pelosi G, Fabbri A, Bianchi F, et al. ΔNp63 (p40) and thyroid transcription factor-1 immunoreactivity on small biopsies or cellblocks for typing non-small cell lung cancer: a novel two-hit, sparing-material approach. *J Thorac Oncol*. 2012;7:281-290.
3. Pelosi G, Rossi G, Cavazza A, et al. ΔNp63 (p40) distribution inside lung cancer: a driver biomarker approach to tumor characterization. *Int J Surg Pathol*. 2013;21:229-239.
4. Borczuk C, Cooper W, Dacic S, et al. *Thoracic Tumours*. Lyon, France: International Agency for Research on Cancer; 2021.
5. Pelosi G, Fabbri A, Tamborini E, et al. Challenging lung carcinoma with coexistent ΔNp63/p40 and thyroid transcription factor-1 labeling within the same individual tumor cells. *J Thorac Oncol*. 2015;10:1500-1502.
6. Hayashi T, Takamochi K, Yanai Y, et al. Non-small cell lung carcinoma with diffuse coexpression of thyroid transcription factor-1 and ΔNp63/p40. *Hum Pathol*. 2018;78:177-181.
7. Spinelli M, Khorshad J, Viola P. When tumor doesn't read textbook. Third case of TTF1 and p40 co-expression in the same tumour cells in a non-small cell carcinoma. A potential new entity to consider? *Pathologica*. 2019;111:58-61.
8. Walia R, Jain D, Madan K, et al. p40 & thyroid transcription factor-1 immunohistochemistry: a useful panel to characterize non-small cell lung carcinoma-not otherwise specified (NSCLC- NOS) category. *Indian J Med Res*. 2017;146:42-48.
9. Forns T, Musick A, Pavlisko E, et al. Dual-staining adenosquamous lung carcinoma with p16 overexpression—a distinct variant? *Mod Pathol*. 2020;33(suppl 1):1772-1773.
10. Travis WD, Brambilla E, Noguchi M, et al. Diagnosis of lung cancer in small biopsies and cytology: implications of the 2011 International Association for the Study of Lung Cancer/American Thoracic Society/European Respiratory Society classification. *Arch Pathol Lab Med*. 2013;137:668-684.

11. Yatabe Y, Dacic S, Borczuk AC, et al. Best practices recommendations for diagnostic immunohistochemistry in lung cancer. *J Thorac Oncol*. 2019;14:377-407.
12. Rekhtman N, Ang DC, Sima CS, Travis WD, Moreira AL. Immunohistochemical algorithm for differentiation of lung adenocarcinoma and squamous cell carcinoma based on large series of whole-tissue sections with validation in small specimens. *Mod Pathol*. 2011;24:1348-1359.
13. Pelosi G, Scarpa A, Forest F, Sonzogni A. The impact of immunohistochemistry on the classification of lung tumors. *Expert Rev Respir Med*. 2016;10:1105-1121.
14. Fumagalli C, Catania C, Ranghiero A, et al. Molecular profile of advanced non-small cell lung cancers in octogenarians: the door to precision medicine in elderly patients. *J Clin Med*. 2019;8:112.
15. Lih CJ, Harrington RD, Sims DJ, et al. Analytical validation of the next-generation sequencing assay for a nationwide signal-finding clinical trial: molecular analysis for therapy choice clinical trial. *J Mol Diagn*. 2017;19:313-327.
16. Yoshida A, Tsuta K, Nakamura H, et al. Comprehensive histologic analysis of ALK-rearranged lung carcinomas. *Am J Surg Pathol*. 2011;35:1226-1234.
17. Caliò A, Nottegar A, Gilioli E, et al. ALK/EML4 fusion gene may be found in pure squamous carcinoma of the lung. *J Thorac Oncol*. 2014;9:729-732.
18. Li Q, Wu J, Yan LX, et al. ALK and ROS1 double-rearranged lung squamous cell carcinoma responding to crizotinib treatment: a case report. *J Thorac Oncol*. 2017;12:e193-e197.
19. Schoenfeld AJ, Chan JM, Kubota D, et al. Tumor analyses reveal squamous transformation and off-target alterations as early resistance mechanisms to first-line osimertinib in EGFR-mutant lung cancer. *Clin Cancer Res*. 2020;26:2654-2663.
20. Cheung AH, Tong JH, Chung LY, et al. EGFR mutation exists in squamous cell lung carcinoma. *Pathology*. 2020;52:323-328.
21. Tanaka Y, Yamaguchi M, Hirai S, et al. Characterization of distal airway stem-like cells expressing N-terminally truncated p63 and thyroid transcription factor-1 in the human lung. *Exp Cell Res*. 2018;372:141-149.
22. Chen X, Chang CW, Spoerke JM, et al. Low-pass whole-genome sequencing of circulating cell-free DNA demonstrates dynamic changes in genomic copy number in a squamous lung cancer clinical cohort. *Clin Cancer Res*. 2019;25:2254-2263.
23. Edelman MJ, Redman MW, Albain KS, et al. SWOG S1400C (NCT02154490)—a phase II study of palbociclib for previously treated cell cycle gene alteration-positive patients with stage IV squamous cell lung cancer (Lung-MAP Substudy). *J Thorac Oncol*. 2019;14:1853-1859.
24. Qian J, Chen R, Zhao R, Han Y, Yu Y. Comprehensive molecular characterizations of Chinese patients with different subtypes of lung squamous cell carcinoma. *Front Oncol*. 2020;10:607130.
25. Redig AJ, Capelletti M, Dahlberg SE, et al. Clinical and molecular characteristics of NF1-mutant lung cancer. *Clin Cancer Res*. 2016;22:3148-3156.
26. Romano RA, Ortt K, Birkaya B, Smalley K, Sinha S. An active role of the DeltaN isoform of p63 in regulating basal keratin genes K5 and K14 and directing epidermal cell fate. *PLoS One*. 2009;4:e5623.
27. Takeuchi T, Tomida S, Yatabe Y, et al. Expression profile-defined classification of lung adenocarcinoma shows close relationship with underlying major genetic changes and clinicopathologic behaviors. *J Clin Oncol*. 2006;24:1679-1688.
28. Liu Y, Nekulova M, Nenutil R, et al. ΔNp63/p40 correlates with the location and phenotype of basal/mesenchymal cancer stem-like cells in human ER+ and HER2+ breast cancers. *J Pathol Clin Res*. 2020;6:83-93.
29. Prat A, Perou CM. Mammary development meets cancer genomics. *Nat Med*. 2009;15:842-844.
30. Schoenfeld AJ, Bandlamudi C, Lavery JA, et al. The genomic landscape of SMARCA4 alterations and associations with outcomes in patients with lung cancer. *Clin Cancer Res*. 2020;26:5701-5708.
31. Fountzilas E, Kurzrock R, Hiep Vo H, Tsimberidou AM. Wedding of molecular alterations and immune checkpoint blockade: genomics as a matchmaker [e-pub ahead of print]. *J Natl Cancer Inst*. https://doi.org/10.1093/jnci/djab067, accessed April 6, 2021.
32. Yu S, Liu D, Shen B, Shi M, Feng J. Immunotherapy strategy of EGFR mutant lung cancer. *Am J Cancer Res*. 2018;8:2106-2115.
33. Wang R, Yamada T, Kita K, et al. Transient IGF-1R inhibition combined with osimertinib eradicates AXL-low expressing EGFR mutated lung cancer. *Nat Commun*. 2020;11:4607.
34. Chang N, Duan J, Wang L, Dong Z, Liu Z. Patients with advanced non-small cell lung cancer with EGFR mutations in addition to complex mutations treated with osimertinib have a poor clinical outcome: a real-world data analysis. *Oncol Lett*. 2020;20:2266-2272.
35. Leonetti A, Sharma S, Minari R, Perego P, Giovannetti E, Tiseo M. Resistance mechanisms to osimertinib in EGFR-mutated non-small cell lung cancer. *Br J Cancer*. 2019;121:725-737.
36. Canale M, Petracci E, Delmonte A, et al. Concomitant TP53 mutation confers worse prognosis in EGFR-mutated non-small cell lung cancer patients treated with TKIs. *J Clin Med*. 2020;9:1047.